Physiological changes of premotor nonspiking interneurons in the central compensation of eyestalk posture following unilateral sensory ablation in crayfish

Kenichi Fujisawa[1] and Masakazu Takahata[2]

[1]Division of Biological Sciences

Graduate School of Science

and

[2]Department of Biological Sciences

Faculty of Science

Hokkaido University

Sapporo 060-0810

Japan

e-mail address: fujisawa@sci.hokudai.ac.jp

tel: +81-11-706-2753

fax: +81-11-706-4923

Running title: Physiological mechanisms underlying central compensation in crustaceans

Keywords: crayfish, statocyst, eyestalk, central compensation, nonspiking giant interneuron

Abstracts

We investigated how the physiological characteristics and synaptic activities of NGIs (Nonspiking Giant Interneurons), which integrate sensory inputs in the brain and send synaptic outputs to oculomotor neurons innervating eyestalk muscles, changed after unilateral ablation of the statocyst in order to clarify neuronal mechanisms underlying the central compensation process in crayfish. The input resistance and membrane time constant in recovered animals that restored the original symmetrical eyestalk posture two weeks after operation were significantly greater than those immediately after operation on the operated side whereas in non-recovered animals only the membrane time constant showed a significant increase. On the intact side, both recovered and non-recovered animals showed no difference. The frequency of synaptic activity showed a complex pattern of change on both sides depending on the polarity of the synaptic potential. The synaptic activity returned to the bilaterally symmetrical level in recovered animals while bilateral asymmetry remained in non-recovered ones. These results suggest that the central compensation of eyestalk posture following unilateral impairment of the statocyst is subserved by not only changes in the physiological characteristics of the NGI membrane but also the activity of neuronal circuits presynaptic to NGIs.

Introduction

Unilateral impairment of the geotactic sense organ immediately causes an abnormal posture that is bilaterally asymmetrical. However, this posture is gradually normalized to restore the original symmetrical posture. The posture compensation following partial destruction of the geotactic sense organ has been well known in many animals including vertebrates (Smith and Curthoys 1989; Darlington and Smith 2000; Dieringer 1995) and invertebrates (Schöne 1954, 1971; Sakuraba and Takahata 1999), the time required for the recovery depending on the animal species, ranging from several hours (rat) to weeks (rabbit). The neuronal mechanisms underlying the behavioral recovery, however, largely remain elusive.

Decapod crustaceans possess a pair of equilibrium sense organs called statocysts. In each statocyst, a statolith that consists of numerous sand grains glued together rests on the sensory hairs and stimulates them when the animal body is tilted (Prentiss 1901). Together with eyes and leg proprioceptors, statocysts are primarily responsible for maintaining and controlling the posture of the animal body and appendages including eyestalks that show compensatory movements in response to body rolling to keep the visual field constant (Schöne 1954; Davis 1971; Mellon and Lorton 1977; Neil 1982). When the statocyst is disabled unilaterally and no leg substratum is provided, the eyestalks take a posture that is bilaterally asymmetrical in the upright (0˚) position. The asymmetrical posture of eyestalks, however, has been known to disappear in several days so that the original symmetrical posture is recovered. This process is called central compensation (Schöne 1954).

The neuronal circuit subserving the eyestalk posture control has been intensively analyzed by many investigators (Wiersma and Yamaguchi 1967; Mellon 1977; Mellon and

Lorton 1977; Yoshino et al. 1983; Nakagawa and Hisada 1992; Hama and Takahata 2005), recently focusing on an identified set of nonspiking interneurons called NGIs (Nonspiking Giant Interneurons) that play the role of premotor neurons in the eyestalk posture control (Okada and Yamaguchi 1988; Yamaguchi and Okada 1990). Furudate et al. (1996) have shown that visual, leg proprioceptive and geotactic inputs converge on NGIs suggesting that they function in integrating sensory inputs to generate oculomotor control signals for the eyestalk posture under natural conditions. Thus NGIs appear to occupy the central position in the neuronal circuit controlling the eyestalk posture.

The present study was undertaken to investigate the neurophysiological mechanisms underlying the behavioral recovery from unilateral statolith removal in the crayfish by quantitatively analyzing the changes in membrane properties and synaptic activity of NGIs throughout the recovery process. This paper specifically aimed to explore whether the membrane time constant, input resistance, and the frequency of spontaneous synaptic activity of NGIs showed any changes depending on whether the animal recovered its original eyestalk posture or not after the statolith was removed unilaterally.

Materials and methods

Animals

Adult crayfish, *Procambarus clarkii* Girard, of both sexes, ranging from 7-10 cm in body length were obtained commercially from local dealers (Sankyo Lab, Sapporo and ME Suisan, Miyagi). They were kept in laboratory tanks until use and fed weekly on a diet of raw potato and liver. There were no significant differences in obtained results between sexes.

Post-operative conditions and statolith removal

The statocyst was disabled by the following procedures. First, the hairs covering the statocyst aperture on the dorsal surface of the antennular basal segment were removed with fine forceps. A jet of water was then directed into the statocyst lumen with a pipette to wash out the statolith. In this experiment, we used animals at four different stages of recovery: before statolith removal, immediately after removal, 14 days after removal when the original symmetrical configuration of bilateral eyestalk was completely recovered, and 14 days after removal when the recovery was partial or completely absent. Operated animals were kept unrestricted so that they could freely move around on the floor of a plastic aquarium (30 × 18 × 25 cm) filled with water (4 cm in depth) under the visual input condition that was bilaterally symmetrical. All animals were reared under a 12:12 light (86 ± 5.9 lux) -dark cycle at room temperature. Continuous illumination was provided by 2 fluorescent tubes (20W) located about 3 m above the aquarium.

Preparations

Before dissection, each crayfish was cooled to 4°C in ice water. Chelipeds and rostrum were removed. The small part of the anterodorsal carapace corresponding to the protogastric area was removed. Gastric juice was sucked out from the stomach with a syringe, and the stomach and green glands were then removed to expose the brain for electrical recording. The cephalothoracic cavity was repeatedly flushed out with cooled crayfish saline (van Harreveld 1936). The circumesophageal commissures were left intact bilaterally for immobilizing the brain during intracellular recording. An aluminum plate was glued to the dorso-anterior region of the cephalothorax. Then the animal was fixed, dorsal-side-up and slightly head-down in the air, to the experimental apparatus by the plate glued onto the cephalothorax.

In order to minize the time for making preparation and to facilitate changing the experimental animal, we did not apply the perfusion technique (Silvey and Sandeman 1976) to the circulatory system to the brain and the eyestalk ganglia. Without the perfusion, the animal usually lost the reflex withdrawal capability of eyestalks due to hypoxia within 30 minutes on average after the preparation for intracellular recording was established. We therefore had to complete physiological experiments as quickly as possible. In order to confirm that the obtained data were trustable, we tested this capability whenever we made successful intracellular recording. The intracellular staining after the physiological experiment, however, was conducted regardless of whether the animal was healthy or not at the end of staining. Physiological data obtained in deteriorated animals were excluded from the data pool for quantitative analyses.

Intracellular recording and current injection

Five pairs of NGIs (G1 - G5) exist just above the protocerebrum bridge in the crayfish brain (Fig. 1A). They have no demonstrable axons, but have large dendritic processes that lie across the midline with short thick primary branches (Fig. 1B). Their somata are located near the surface of the distal end of the optic tract (Okada and Yamaguchi 1988). For intracellular recording and current injection, quartz glass microelectrodes filled with 3% solution of Lucifer yellow CH (Stewart 1978) in 1M lithium chloride were employed. The NGI was impaled with the microelectrode on or near the midline. The electrode had DC resistance of 10 - 20 MΩ in the saline and could pass current of either direction without noticeable change in the electrode resistance. It was coupled to a high input impedance amplifier (Nihon-Kohden CZ-3100) whose output was directed to a storage oscilloscope (Tektronix 5100) and a digital data recorder (Bio-Logic DTR-1801). A penetrated cell was identified as one of the NGIs by (1) the presence of a spontaneous fluctuation in the membrane potential due to synaptic activities and (2) characteristic responses to illumination of the compound eyes (Okada and Yamaguchi 1988). Final identification of the cell was based on its morphology. The data obtained from NGIs G4 and G5 were excluded from the present analyses since they constitute a morphologically different cluster from that constituted of G1, G2 and G3.

Once the resting potential was observed to stabilize in the continuous current clamp mode, the amplifier was switched to the discontinuous current clamp mode in which the single electrode was rapidly switched between the current injection and voltage recording circuits. This method requires that the switching frequency for voltage sampling be low enough compared with the recovery time of the microelectrode following current injection, and high enough relative to the time constant of the cell (Finkel and Redman 1985; Wilson

and Goldner 1975). In order to attain a high switching frequency, the stray capacitance of the microelectrode to the ground created by glass wall/saline interfaces was reduced by using quartz glass microelectrodes, which created lower stray capacitance compared with the borosilicate. The optimal capacitance compensation of the recording system was obtained by monitoring the voltage across the microelectrode with an additional oscilloscope. The sampling frequency we could use in the discontinuous mode was 1.0 - 2.0 kHz. Constant current (1-5 nA in intensity, 160ms in duration) was injected into the cell through the electrode using the discontinuous current clamp mode of the amplifier.

The input resistance and the membrane time constant of NGIs were obtained from their voltage responses to intracellular injection of step current pulses of -1 nA. The voltage response to current injection was recorded 32 - 64 times and all responses were digitized and averaged to obtain a mean value on a digital oscilloscope (Iwatsu DS-9121) so that the membrane potential fluctuation due to spontaneous synaptic activities was minimized. The input resistance was obtained by dividing the steady-state voltage change by the amount of injected current. The membrane time constant was extracted from the transient voltage response by the graphical peeling method (Rall 1969). The voltage response of NGIs in this study could be expressed as a sum of two exponentials with different time constants. The slower time constant represented the membrane time constant whereas the faster one represented the equalizing time constant that was associated with rapid reduction of voltage differences between different membrane regions (Rall et al. 1992).

After the physiological experiments were completed, Lucifer yellow was injected electrophoretically into the impaled cell by applying 8 - 10 nA hyperpolarizing current

pulses of 500 ms duration at 1 Hz for about 15 - 30 minutes. After completion of dye injection, the resting potential was measured as the voltage difference between before and after the electrode withdrawal from the cell. The brain was immediately dissected and fixed in 10% formalin for 30 minutes, followed by dehydration in an alcohol series (10 minutes respectively in 80%, 90% and 100%) and cleared in methylsalicylate. The cleared ganglion was examined under a Nikon Optiphoto 2 epifluorescence microscope (Tokyo, Japan).

Statolith removal during intracellular recording

In some experiments, the membrane potential of an NGI was recorded continuously throughout the water jet process to study the synaptic responses caused by statolith elimination. Before the experiment, a nozzle joined with a syringe by a polyethylene tube was fixed to the experimental apparatus in a position just above the statocyst lumen of crayfish. The nozzle and the animal could be manually rotated as one set during the preparation set-up. They were finally kept at a tilted position most appropriate for microelectrode approach to the brain. Once a microelectrode penetrated one of the NGIs, the statolith was removed on one side by water jet from the nozzle during intracellular recording. The membrane conductance change due to the statolith removal was studied by intracellularly injecting a small constant-current pulses into the cell to measure its voltage responses.

Results

NGIs spontaneously show depolarizing and hyperpolarizing synaptic potentials without any stimulus (Fig. 1C). Experimental alteration of their membrane potential by intracellular current injection causes either an increase or a decrease in the eyecup muscle activity depending on the direction of the membrane potential change (Fig. 1D). The input and output connections of NGIs proposed by Okada et al. (1994) are summarized in Fig. 1E. The resting potential of NGIs measured in this study ranged from -44 to -65 mV in intact animals.

Resting potenital

When the statolith was removed on the opposite side to the cell body, the resting potential of the NGI shifted toward depolarization (≈3 mV; Fig. 2A) whereas it moved toward hyperpolarization (≈5 mV) when the statolith was removed on the same side with the cell body (Fig. 2B). The depolarization caused by statolith removal on the opposite side was found to be associated with an increase in the membrane conductance (Fig. 2C). It was noted here that the frequency of spontaneous hyperpolarizing synaptic potentials decreased following the statolith removal (see below). These changes on the resting potential of NGIs following the unilateral statolith removal, however, turned out to be statistically insignificant. The average resting potential on the intact and operated side at the four different stages are compared in Fig. 3. It showed no statistically significant difference between the right (-54.6 ± 0.9; mean ± standard error, N =12) and left (-54.8 ± 2.1, N = 10) NGIs in intact animals. Data obtained on both sides were therefore pooled together when the resting potential was to be compared with that recorded at other three stages following

the unilateral statolith removal. No significant difference was detected in the resting potential between the operated and intact side (Student's two-sided t-test for unpaired comparison, P>0.05). The resting potential of NGIs was -55.8 ± 1.2 mV (N = 13) and -56.9 ± 1.4 mV (N = 10) on the operated and intact side respectively 1 hour after operation. It was -56.3 ± 1.7 mV (N = 11) on the operated side and -55.7 ± 1.4 mV (N = 19) on the intact side 14 days after operation in non-recovered animals. In recovered animals, it was -53.2 ± 1.7 mV (N = 10) and -56.2 ± 1.7 mV (N = 11). On both sides, no significant difference was observed in the resting potential between intact animals, those 1 hour after operation, recovered and non-recovered animals 14 days after operation. Although the resting potential was confirmed to change following the statocyst removal on either side (Fig. 2), the result of statistical analyses (Fig. 3) indicated that the resting potential remained unchanged before and after the unilateral statolith removal. This discrepancy was partly due to the small amplitude of potential changes following the operation compared with the large variability in the resting potential among different animals.

Input resistance and membrane time constant

When constant current pulses (-5 nA - +5 nA) were injected into NGIs, their dendritic membrane showed outward rectification upon depolarization. This rectification was maintained throughout the recovery course (Fig. 4A1-3). The input resistance and membrane time constant of NGIs were obtained from their voltage responses to injection of a hyperpolarizing step current (-1 nA) at the resting potential level where the membrane of NGIs behaved passively. In intact crayfish, there was no significant difference (P > 0.05) in the input resistance of NGIs between the right (6.3 ± 0.6 MΩ, N =14) and left (5.5 ± 0.6

MΩ, N = 11) side (Fig. 4B). The input resistance of NGIs on both sides in total was 6.0 ± 0.4 MΩ (N = 25). One hour after operation, the input resistance was 4.9 ± 0.6 MΩ (N = 15) and 5.4 ± 0.8 MΩ (N =14) on the operated and intact side respectively. There was a slight reduction in input resistance after the statolith removal on either side, but the difference was not significant ($P > 0.05$). In non-recovered animals 14 days after operation, the input resistance was 6.2 ± 0.7 MΩ (N = 19) on the operated side and 5.6 ± 0.6 MΩ (N = 15) on the intact side. In recovered animals, the input resistance was 7.8 ± 1.1 MΩ (N = 12) on the operated side and 6.9 ± 0.8 MΩ (N = 12) on the intact side. The input resistance on the operated side showed significantl difference between recovered animals and those 1 hour after operation ($P < 0.05$). The difference was not significant in non-recovered animals on the operated side and both recovered and non-recovered animals on the opposite side.

The membrane time constant was 16.1 ± 1.1 msec (N = 25) in total of both sides in intact animals (Fig. 4C). One hour after statolith removal, it was 12.7 ± 1.5 msec (N = 15) on the operated side and 14.3 ± 1.5 msec (N = 14) on the intact side. Non-recovered animals showed 17.7 ± 1.6 msec (N = 19) on the operated side and 16.6 ± 1.9 msec (N = 15) on the intact side, whereas recovered animals showed 20.9 ± 3.0 msec (N = 12) and 18.6 ± 2.1 msec (N = 15) on the operated and intact side respectively. Compared with the animals 1 hour after operation, a significant increase ($P < 0.05$) in the membrane time constant was observed in both non-recovered and recovered animals on the operated side. No significant change was observed on the opposite side.

Comparison of the input resistance and membrane time constant values between the operated and intact side revealed no significant differences ($P > 0.05$) 1 hour and 14 days

after statolith removal regardless of whether the animal restored the original symmetrical posture of eyestalks or not, although their post-operative changes were significantly asymmetrical ($P < 0.05$). Thus, statistically, the bilateral balance of passive membrane properties was maintained in both the pre- and post-operative period.

Spontaneous synaptic activity

NGIs showed a spontaneous fluctuation in the membrane potential even when no specific stimulus was present (Fig. 1C), although bilaterally balanced general stimuli were present for statocysts, eyes and leg proprioceptors. This fluctuation consisted of discrete depolarizing and hyperpolarizing postsynaptic potentials (PSPs). In order to compare quantitatively the spontaneous synaptic activity of NGIs in intact and operated animals, the number of these depolarizing and hyperpolarizing PSPs was counted and expressed as the frequency per second (Fig. 5). The peak amplitude of these potentials varied from 0.9 to 11.8 mV in depolarizing PSPs, and from 0.8 to 13.9 mV in hyperpolarizing ones. In the present study, the frequency of depolarizing and hyperpolarizing PSPs was measured regardless of their peak amplitude. In intact animals, the frequency of depolarizing (23.5 ± 2.4 Hz on the right and 25.8 ± 1.9 Hz on the lest side) and hyperpolarizing (22.3 ± 1.9 Hz and 22.4 ± 2.0 Hz) PSPs was nearly the same on both sides ($P > 0.05$). In the following comparison, the data from the right and left side were pooled together to represent the PSP frequency in intact animals.

When the statolith was removed unilaterally, the frequency of depolarizing PSPs increased while the frequency of hyperpolarizing PSPs decreased on the intact side (Fig. 5A1) whereas, on the operated side, the frequency of depolarizing PSPs did not change

while the frequency of hyperpolarizing PSPs increased (Fig. 5A2). The postoperative change in the PSP frequency is summarized for comparison in Fig. 5B (depolarizing PSPs) and C (hyperpolarizing PSPs). One hour after the statolith removal, the frequency of depolarizing PSPs on the intact side (37.5 ± 3.1 Hz) increased significantly from that observed in intact animals (24.7 ± 1.5 Hz, $P < 0.05$) (Fig. 5B), whereas the frequency of hyperpolarizing PSPs (8.0 ± 1.7 Hz) decreased significantly from that of intact animals (22.3 ± 1.3 Hz, $P < 0.05$) (Fig. 5C). On the operated side, there were no statistically significant changes in the PSP frequency between intact (22.8 ± 3.2 Hz) and operated animals (26.9 ± 1.9 Hz) (Fig. 5B, C). When they showed no recovery in the eyestalk posture 14 days after operation, the frequency of hyperpolarizing PSPs (17.0 ± 2.3 Hz on the operated and 11.3 ± 1.3 Hz on the intact side) was statistically lower than the normal level on both sides ($P < 0.05$) (Fig. 5C), although the frequency of depolarizing PSPs (21.6 ± 2.1 Hz and 24.9 ± 2.8 Hz, respectively) returned to the normal level (Fig. 5B). When the animals showed recovery, the frequencies of depolarizing and hyperpolarizing PSPs (18.0 ± 1.4 Hz and 16.7 ± 1.7 Hz respectively) were statistically lower than the normal level on the operated side (Fig. 5B, C). By contrast, on the intact side, the frequencies of depolarizing and hyperpolarizing PSPs (19.4 ± 2.7 Hz and 17.4 ± 2.1 Hz respectively) were statistically not different from the normal level (Fig. 5B, C).

The synaptic activities, both depolarizing and hyperpolarizing, were balanced bilaterally in intact animals. One hour after the operation, the frequency of depolarizing PSPs on the intact side (37.5 ± 3.1 Hz) was higher ($P < 0.05$) than that on the operated side (22.8 ± 3.2 Hz). By contrast, the frequency of hyperpolarizing PSPs on the intact side (8.0 ± 1.7 Hz) was lower ($P < 0.05$) than that on the operated side (26.9 ± 1.9 Hz). Fourteen

days after operation, the frequency of hyperpolarizing PSPs on the intact side (11.3 ± 1.3 Hz) was lower than that on the operated side (17.0 ± 2.3 Hz) in non-recovered animals ($P < 0.05$). The frequency of depolarizing PSPs was not statistically different between both sides. The results showed that the imbalance of synaptic activity observed 1 hour after operation was not canceled completely in non-recovered animals. In recovered animals, although the frequency of depolarizing and hyperpolarizing PSPs on both sides slightly reduced from the normal level, there was no significant difference in the frequency of depolarizing (18.0 ± 1.4 Hz on the operated and 19.4 ± 2.7 Hz on the intact side) and hyperpolarizing (17.0 ± 2.3 Hz and 11.3 ± 1.3 Hz, respectively) PSPs between both sides ($P > 0.05$). Hence, in intact and recovered animals, both the depolarizing and hyperpolarizing synaptic activities on both sides are balanced in their frequency. These results indicate that the changes in the frequency of spontaneous PSPs are consistent with the eyestalk deviation observed at each stage of recovery from the unilateral statolith removal, suggesting the possibility that the recovery of the original eyestalk posture is based on restoration of the symmetry in the synaptic activities on both sides (see Discussion).

Shape parameters of spontaneous PSPs

In intact animals, the peak amplitude of depolarizing PSPs was 3.98 ± 0.11 mV and that of hyperpolarizing PSPs was 3.67 ± 0.14 mV. One hour after statolith removal, the peak amplitude of depolarizing and hyperpolarizing PSPs showed a significant increase on the intact side (4.67 ± 0.14 mV; $P < 0.05$) and on the operated side (4.45 ± 0.21 mV; $P < 0.05$) respectively from the normal level. In non-recovered animals, except depolarizing

PSPs on the operated side, the peak amplitude of PSPs became smaller than the normal level ($P < 0.05$). In recovered animals, the amplitude of depolarizing and hyperpolarizing PSPs was smaller than the normal level ($P < 0.05$) on both sides. Thus the peak amplitude of spontaneous depolarizing and hyperpolarizing PSPs was balanced in intact animals whereas in operated and non-recovered animals it was not balanced (Fig. 6A1, 2). In recovered animals, the hyperpolarizing PSPs were balanced, but the depolarizing ones remained bilaterally imbalanced.

The rate of rise of PSPs in each recovery stage was obtained by dividing the peak amplitude by the time from the onset of a PSP to its peak. In intact animals, the depolarizing PSPs had a higher rise rate than the hyperpolarizing PSPs (1.15 ± 0.04 mV/msec and 0.81 ± 0.03 mV/msec respectively), but both were balanced bilaterally. One hour after operation, the rise rate of depolarizing PSPs showed a significant increase ($P < 0.05$) on the operated (1.77 ± 0.14 mV/msec) and intact (2.22 ± 0.12 mV/msec) side. The rise rate of hyperpolarizing PSPs showed an increase only on the operated side (1.05 ± 0.05 mV/msec; $P < 0.05$). In non-recovered animals, the rise rate of depolarizing PSPs remained higher than the normal level ($P < 0.05$) on the operated (1.95 ± 0.09 mV/msec) and intact (1.53 ± 0.08 mV/msec) side. By contrast, the rise rate of hyperpolarizing PSPs showed a decrease from the normal level ($P<0.05$) on the operated (0.52 ± 0.04 mV/msec) and intact side (and 0.23 ± 0.02 mV/msec). In recovered animals, there was no significant change from the normal level in the rise rate of depolarizing (1.30 ± 0.09 mV/msec) and hyperpolarizing PSPs (0.71 ± 0.03 mV/msec) on the operated side. However, the rise rate of depolarizing (0.94 ± 0.04 mV/msec) and hyperpolarizing PSPs (0.61 ± 0.04 mV/msec) decreased significantly from the normal level on the intact side ($P < 0.05$). In sum, the rise

rate of depolarizing and hyperpolarizing PSPs was balanced bilaterally in recovered animals, but not in non-recovered animals (Fig. 6B1, 2).

The half decay time of PSPs was obtained by measuring the period from the onset of a PSP to the time when the PSP decayed to the half of the peak amplitude. In intact animals, the half decay time of depolarizing PSPs was 9.63 ± 0.22 msec and that of hyperpolarizing PSPs was 11.76 ± 0.27 msec. One hour after operation, the depolarizing PSPs showed a statistically shorter half decay time than the normal level on the operated and intact side (7.84 ± 0.29 msec and 7.98 ± 0.22 msec respectively; $P<0.05$). These significant differences remained in non-recovered animals. In recovered animals, these differences disappeared and the half decay time of depolarizing PSPs showed no significant difference from the normal level on both sides. The half decay time of hyperpolarizing PSPs showed a decrease from the normal level on the intact side (10.33 ± 0.63 msec; $P < 0.05$) 1 hour after operation. This shorter half decay time remained in non-recovered and recovered animals. On the operated side, the half decay time of hyperpolarizing PSPs showed a decrease in non-recovered animals (9.70 ± 0.34 msec; $P < 0.05$) from the normal level. The hyperpolarizing PSPs also showed a shorter half decay time than the normal level in recovered animals (10.59 ± 0.39 msec; $P < 0.05$). One hour after operation, the half decay time of hyperpolarizing PSPs (11.17 ± 0.31 msec) did not change from the normal level ($P > 0.05$). The half decay time of depolarizing and hyperpolarizing PSPs were thus balanced bilaterally in intact, recovered and non-recovered animals (Fig. 6C1, 2) as well as in those 1 hour after operation.

Discussion

Bilateral symmetry in the eyestalk posture is maintained by balanced activities of the eyestalk motor system on each side. The eyestalk posture is controlled by 10 (Sugawara et al. 1971) or 11 (Mellon 1977) muscles that are innervated by three populations of oculomotor neurons (Hisada and Higuchi 1973; Mellon et al. 1976; Mellon 1977). They are in turn partly controlled by a set of identifiable premotor nonspiking interneurons called NGIs (Okada and Yamaguchi 1988). When the statolith is removed unilaterally, the eyestalks immediately show bilateral asymmetry. This asymmetrical posture gradually disappears so that the original eyestalk posture is restored in a few weeks (Schöne 1954, 1971). We found that this recovery called central compensation depends on the postoperative sensory condition (Sakuraba and Takahata 1999, 2000): bilateral leg proprioceptive inputs were critically required for the recovery of symmetrical eyestalk posture after unilateral statolith removal. In order to understand the neuronal mechanism underlying the central compensation of eyestalk posture following the unilateral removal of statolith, it is important to examine how the physiological properties and activities of NGIs change after the operation.

The results obtained in this study are summarized schematically in Fig. 7 with special reference to the bilateral balance of NGI activities. After unilateral statolith removal, both the input resistance and membrane time constant significantly increased on the operated side in those animals that recovered the original symmetrical eyestalk posture whereas only the membrane time constant showed a significant increase on the operated side in non-recovered animals from the level observed in those 1 hour after operation (Fig. 4). Consequently, the passive membrane properties were balanced between the operated and

intact side in both the recovered and non-recovered animals. The spontaneous synaptic activities showed bilateral asymmetry immediately after unilateral statolith removal. This asymmetry completely disappeared in recovered animals, but partially remained in non-recovered animals 14 days after the operation (Fig. 5). The shape indices of unitary depolarizing and hyperpolarizing PSPs also showed bilateral asymmetry right after operation. This asymmetry disappeared only in recovered animals except the half decay time which was balanced in both recovered and non-recovered animals (Fig. 6). In the following sections, we discuss the physiological significance of these changes and possible mechanisms subserving the compensation.

Resting potential, input resistance and membrane time constant

When a statolith was removed by water jet during intracellular recording, the membrane was slightly depolarized or hyperpolarized depending on which side the statolith was removed (Fig. 2). One hour after operation, this difference was not statistically significant (Fig. 3; $P > 0.05$) probably due to the large variability in the resting potential among preparations. No noticeable change was observed in the resting potential throughout the post-operative period (Fig. 3). Since nonspiking interneurons directly control the postsynaptic neuron activity by their membrane potential (Burrows and Siegler 1978; Burrows 1979; Siegler 1981), it was first expected that the resting potential of NGIs would change in parallel with the eyestalk motor neuron activity during the central compensation process. This expectation, however, was negated by the present observation.

The input resistance and membrane time constant of NGIs tended to show an increase from the normal level after operation. This tendency was more remarkable on the operated

side than on the intact side. However, the increase was not statistically significant ($P > 0.05$). In those animals that restored the original symmetrical eyestalk posture 14 days after operation, both the input resistance and membrane time constant showed a significant increase from the level observed 1 hour after the statolith removal on the operated side ($P < 0.05$). No significant change was observed on the intact side. Consequently, the input resistance and membrane time constant values on the operated side were larger than those on the intact side (Fig. 7). In non-recovered animals, only the membrane time constant was imbalanced, greater on the operated side than on the intact side. These findings suggest that the increase in the input resistance and membrane time constant of NGIs on the operated side is responsible, at least partly, for the restoration of original symmetrical configuration of bilateral eyestalks in the course of central compensation.

The input resistance is dependent on two major factors: the membrane resistance per unit area and the dendritic morphology (Rall 1981). We used a confocal laser scanning microscope to examine the fine structure of NGI dendrites. No morphological change was noticed during the compensation process although no quantitative analysis was carried out. We tentatively concluded that the increase in input resistance was due to an increase in the membrane resistance per unit area, i.e., the specific membrane resistance. This conclusion is consistent with our observation that the membrane time constant, defined as the product of membrane resistance and capacitance per unit area where the capacitance is considered to be constant (Rall et al. 1992), showed an increase (Fig. 4C) in association with the input resistance (Fig. 4B), although an increase in the membrane time constant was not associated with any significant change in the input resistance in non-recovered animals (Fig. 4B). It should be noted here, however, that the input resistance showed a tendency of

increase in these animals, although it was not statistically significant. We think that the increase in the specific membrane resistance remained insufficient in non-recovered animals so that the input resistance values showed considerable variances. Consequently, our statistical analysis could not reveal any significant change in the input resistance while barely revealing a significant change in the membrane time constant. The increase in input resistance and membrane time constant would enhance the amplitude and time course of synaptic potentials as long as those of the synaptic current that is caused by a certain amount of neurotransmitter molecules released from presynaptic neurons are not changed. The functional significance of this increase, however, remains to be further studied.

Spontaneous synaptic input

The effect of unilateral statolith removal on the spontaneous synaptic activity was observed more remarkably on the intact side than on the operated side. The frequency of excitatory depolarizing PSPs significantly increased whereas that of inhibitory hyperpolarizing PSPs decreased from the normal level on the intact side following the statolith removal (Fig. 5). The synaptic activity was less affected on the operated side. Consequently, a significant imbalance in excitatory and inhibitory synaptic input was present between bilateral NGIs right after the statolith removal. As summarized in Fig. 7, this imbalance was completely canceled in recovered animals whereas it partially remained in non-recovered animals. It should be noted here that the balanced frequency in recovered animals was significantly lower than that in intact animals for both excitatory and inhibitory input (Fig. 5). Since the bilateral symmetry in eyestalk posture is based on the symmetry of synaptic input rather than its intensity, the decrease in the balanced activity

level has no functional significance in maintaining the symmetrical posture. It remains to be studied, however, if the lowered synaptic activity has any functional significance in the restoration of the initial symmetrical posture of bilateral eyestalks.

The fact that the frequency of spontaneous PSPs changed significantly in the course of central compensation suggests that the crucial site of change associated with the eyestalk posture recovery is located in the presynaptic pathway to NGIs in addition to themselves since the PSP frequency reflects the spike activity of those neurons presynaptic to NGIs. Many spiking local interneurons have been identified (Nakagawa and Hisada 1992) that respond to the statocyst stimulation by artificial bending of sensory hairs. They extend neurites in the protocerebrum where NGIs are located (Okada and Yamaguchi 1988) and the deutocerebrum where statocyst afferents project (Yoshino et al. 1983). It is expected that these local interneurons mediate statocyst information to NGIs, but further study is needed to clarify which interneurons are presynaptic to NGIs and how many interneurons are involved in the circuit presynaptic to NGIs.

Peak amplitude, rise rate and half decay time of PSPs

Changes in the shape of synaptic potentials have been reported in the vestibular compensation process of frogs (Dieringer and Precht 1977, 1979a,b; Galiana et al. 1984), although the physiological mechanism underlying those changes remains unknown. In the present study, we found that the peak amplitude of excitatory and inhibitory PSPs as well as their rise rate and half decay time showed complex changes depending on the polarity and laterality (Fig. 6). The only observation that appeared to be relevant to the central compensation was the symmetry of these shape parameters in intact and recovered animals.

One hour after operation, the peak amplitude and rise rate were bilaterally asymmetrical for both excitatory and inhibitory PSPs. These asymmetries were canceled in recovered animals except that of the excitatory PSP amplitude while they all remained as they were 1 hour after operation in non-recovered animals. The balanced level of the rise rate and half decay time in recovered animals was in general comparable with that in intact animals, although in some cases the difference in the balanced level was statistically significant (Fig. 6).

The peak amplitude of PSPs in NGIs depends on two possible factors: the input resistance of NGI and the amount of neurotransmitter release from presynaptic terminals. The input resistance of NGI significantly increased after unilateral statolith removal only on the operated side (Fig. 4). The bilateral symmetry in the peak amplitude of PSPs under such an asymmetrical condition in the input resistance suggests that the amount of neurotransmitter release from the presynaptic neuron is asymmetrical, greater on the side with a lower input resistance value than on the side with a higher one. Thus the central compensation process that restores the original symmetrical posture of eyestalks appears to involve asymmetrization of neurotransmitter release from presynaptic neurons to NGIs. It is unknown at present, however, what mechanism subserves the change in the neurotransmitter release. It is unlikely, in any case, that the recovery of symmetrical eyestalk posture is directly correlated with any change in the shape indices of spontaneous PSPs of NGIs following the statolith removal.

Possible mechanisms of central compensation

Both in intact animals and in those which restored the original eyestalk posture after

unilateral statolith removal, the muscle activity for eyestalk posture control is bilaterally balanced (Sakuraba and Takahata 2000) and hence the motor neuron activity responsible for controlling the eyestalk muscle activity is also bilaterally balanced. The bilateral balance was also held in the input resistance and membrane time constant of NGIs in both the pre- and post-operative animals (Fig. 4). It should be noted here that the input resistance and membrane time constant showed a significant increase after the unilateral statolith removal only on the operated side in recovered animals. In non-recovered animals, only the membrane time constant showed a significant increase on the operated side. As discussed above, we tentatively conclude that the bilateral balance of passive membrane properties in the recovered animals was attained by a sufficient, but bilaterally asymmetrical, increase in the specific membrane resistance. On the other hand, the synaptic input to NGIs became bilaterally asymmetrical following the operation, but was balanced in recovered animals as well as in intact animals (Fig. 5). These findings and considerations indicate that the central compensation is subserved by changes in not only NGIs themselves but also their presynaptic neurons involving both symmetrization and asymmetrization of physiological properties, thus based on changes occurring at multiple sites in the statocyst-to-motor neuron pathways.

The result of our intracellular recording demonstrated that the synaptic input to NGIs was affected depending on which of the contralateral or ipsilateral statolith was removed (Fig. 2), indicating that the statocyst afferent activity was imbalanced by unilateral statolith removal. Therefore, a possible explanation for the restoration of the bilateral symmetry would be that the spike activity of statocyst sensory neurons was symmetrized on both sides by some unknown mechanism. This possibility is unlikely, however, because an

efferent control system of the statocyst sensory neuron activity as reported in the molluscan statocyst (Budelmann 1977; Williamson 1989) and in the vertebrate vestibular organ (Klinke and Galley 1974; Highstein and Baker 1985) has never been demonstrated in crustaceans, although we cannot exclude the possibility that some unknown cellular mechanisms might cause hyperactivity of the sensory neurons involved. Furthermore, we reported previously that the leg proprioceptive inputs were critical for the recovery of symmetrical eyestalk posture after unilateral statolith removal (Sakuraba and Takahata 1999): the compensation occurred even when the operated animals were kept in complete darkness provided with a leg substratum, but never occurred without it. Considering the critical role of leg proprioceptive input in the central compensation, it seems to be most plausible that the activity of statocyst-to-motor neuron pathways on both sides is symmetrized with the aid of leg proprioceptor input. Clarification of the site of convergence for statocyst and leg proprioceptor inputs will be hence critical for understanding neuronal mechanisms underlying the central compensation.

In mammals, the unilateral labyrinthectomy induces immediate and severe disabling in the control of resting position of the body, the head, and the gaze (Schaefer et al. 1979; Smith and Curthoys 1989). Over time, this vestibular syndrome abates in the recovery process known as "vestibular compensation" (Smith et al. 1986; Smith and Curthoys 1989; Deliagina 1997). At the neural level, it has been reported repeatedly that the resting discharge of the ipsilateral vestibular nuclei neurons becomes silent while that of contralateral ones increases just after unilateral labyrinthectomy. After a short period, this asymmetry disappears and the behavioral syndromes caused by unilateral labyrinthectomy diminish in parallel with the physiological recovery. (Hamann and Lannou 1987; Smith

and Curthoys 1988a,b; Ris et al. 1995, 1997; Newlands and Perachio 1990a, b). To explain this physiological recovery of bilaterally symmetrical resting discharge, Vibert and his colleagues (1999) proposed that the vestibular compensation follows a "top-down" strategy: it would first rely on the external cues given by the intact sensor systems, then on an internal reorganization of the vestibular-related networks, and finally on changes in the intrinsic pacemaker properties of the vestibular neurons themselves.

The finding in crayfish that the presence of bilateral leg proprioceptive input is primarily required for the recovery of symmetrical eyestalk posture following unilateral statolith removal (Sakuraba and Takahata 1999) suggests a possibility that the activity of neurons presynaptic to NGIs will be modified by leg proprioceptive input at first. This could further cause reorganization of the presynaptic neuron circuit to produce bilaterally symmetrical output to NGIs as in the "top-down" strategy in mammals. However, it remains unknown in both vertebrates and invertebrates how such reorganization is carried out at the neuronal level. The crustacean eyestalk system would be advantageous in analyzing the neuronal mechanisms underlying the "top-down" strategy since the major neuronal components involved in the compensation have been individually identified (Nakagawa and Hisada 1992; Hama and Takahata 2005).

Acknowledgments

We thank Dr. N. Hama for helpful comments and suggestions. We also gratefully acknowledge anonymous reviewers for their constructive criticisms and suggestions. This work was supported in part by a Grant-in-Aid for Scientific Research (No.17370024) from the Ministry of Education, Culture, Sports, Science and Technology of Japan.

References

Budelmann BU (1977) Structure and function of the angular acceleration receptor systems in the statocysts of cephalopods. Symp Zool Soc Lond 38: 309–324

Burrows M (1979) Synaptic potentials effect the release of transmiter from locust nonspiking interneurons. Science 204: 81-83

Burrows M, Siegler MVS (1978) Graded synaptic transmission between local interneurones and motoneurones in the metathoracic ganglion of the locust. J Physiol 285: 231-255

Darlington CL, Smith PF (2000) Molecular mechanisms of recovery from vestibular damage in mammals: recent advances. Prog Neurobiol 62: 313-325

Davis WJ (1971) The integrative action of the nervous system in crustacean equilibrium reactions. In: Gordon SA, Cohen MJ (ed) Gravity and the Organism. Chicago University Press, Chicago, pp 237–250

Deliagina TG (1997) Vestibular compensation in lampreys: Impairment and recovery of equilibrium control during locomotion. J Exp Biol 200: 1459–1471

Dieringer N (1995) Vestibular compensation: Neural plasticity and its relations to functional recovery after labyrinthine lesions in frogs and other vertebrates. Prog Neurobiol 46: 97–129

Dieringer N, Precht W (1977) Modification of synaptic input following unilateral labyrinthectomy. Nature London 296: 431-433

Dieringer N, Precht W (1979a) Mechanisms of compensation for vestibular deficits in the frog. I. Modification of the excitatory commissural system. Exp Brain Res 36: 311-328

Dieringer N, Precht W (1979b) Mechanisms of compensation for vestibular deficits in the

frog. II. Modification of the inhibitory Pathways. Exp Brain Res 36: 329-357

Finkel AS, Redman SJ (1985) Optimal voltage clamping with single microelectrode. In: Smith Jr TG, Lecar H Redman SJ, Gage PW (ed) Voltage and Patch Clamping with Microelectrodes. Am Physiol Soc, Bethesda MD, pp95-120

Furudate H, Okada Y, Yamaguchi T (1996) Responses of non-spiking giant interneurons to substrate tilt in the crayfish, with special reference to multisensory control in the compensatory eyestalk movement system. J Comp Physiol A 179: 635–643

Galiana HL, Flohr H, Jones GM (1984) A reevaluation of intervestibular nuclear coupling: its role in vestibular compensation. J Neurophysiol 51: 242-259.

Hama N, Takahata M (2005) Modification of satatocyst input to local interneurons by behavioral condition in the crayfish. J Comp Physiol A 191: 747-759

Hamann KF, Lannou J (1987) Dynamic characteristics of vestibular nuclear neurons responses to vestibular and optokinetic stimulation during vestibular compensation in the rat. Acta Otolaryngol Suppl 445: 1-19.

Highstein SM, Baker R (1985) Action of the efferent vestibular system on primary afferents in the toadfish, *Opsanus tau*. J Neurophysiol 54: 370–384

Hisada M, Higuchi T (1973) Basic response pattern and classification of oculomotor nerve in the crayfish, *Procambarus Clarkii*. J Fac Sci Hokkaido Univ Ser VI Zool 18(4): 481-494

Klinke R, Galley N (1974) Efferent innervation of vestibular and auditory receptors. Physiol Rev 54:316–357

Mellon DeF (1977) The anatomy and motor nerve distribution of the eye muscles in the crayfish. J Comp Physiol 121: 349-366

Mellon DeF, Tufty RM, Lorton ED (1976) Analysis of spatial constancy of oculomotor neurons in the crayfish. Brain Res 109: 587-954

Mellon DeF, Lorton ED (1977) Reflex actions of the functional divisions in the crayfish oculomotor system, J Comp Physiol A 121: 367-380

Nakagawa H, Hisada M (1992) Local spiking interneurons controlling the equilibrium response in the crayfish *Procambarus clarkii*. J Comp Physiol A 170: 291-302.

Neil DM (1982) Compensatory eye movements. In: Sandeman DC, Atwood HL (ed) The Biology of Crustacea. Vol 4. Academic Press, New York, pp 133–163

Newlands SD, Perachio AA (1990a) Compensation of horizontal canal related activity in the medial vestibular nucleus following unilateral labyrinth ablation in the decerebrate gerbil. I. Type I neurons. Exp Brain Res 82: 359-372.

Newlands SD, Perachio AA (1990b) Compensation of horizontal canal related activity in the medial vestibular nucleus following unilateral labyrinth ablation in the decerebrate gerbil. II. Type II neurons. Exp Brain Res 82: 373-383.

Okada Y, Yamaguchi T (1988) Nonspiking giant interneurons in the crayfish brain: morphological and physiological characteristics of the neurons postsynaptic to visual interneurons. J Comp Physiol A 162: 705–714

Okada Y, Furudate H, Yamaguchi T (1994) Multimodal responses of the nonspiking giant interneurons in the brain of the crayfish Procambarus clarkii. J Comp Physiol A 174: 411-419

Prentiss CW (1901) The otolith of decapode crustacea. Bull Mus Comp Zool Harvard 36: 167-254

Rall W (1969) Time constants and electronic length of membrane cylinders and neurons.

Biophys J 9: 1483-1508

Rall W (1981) Functional aspects of neuronal geometry. In: Roberts A, Bush BMH (ed) Neurones without impulses. Cambridge University Press, Cambridge pp.223-254

Rall W, Burke RE, Holmes WR, Jack JJR, Redman SJ, Segev I (1992) Matching dendritic neuron models to experimental data. Physiol Rev (Suppl) 72: 159-186

Ris L, De Waele C, Serafin M, Vidal PP, Godaux E (1995) Neuronal activity in the ipsilateral vestibular nucleus following unilateral labyrinthectomy in the alert guinea pig. J Neurophysiol 74: 2087-2099

Ris L, Capron B, De Waele C, Vidal PP, Godaux E (1997) Dissociations between behavioural recovery and restoration of vestibular activity in the unilabyrinthectomized guinea pig. J Physiol (Lond) 500: 509-522

Sakuraba T, Takahata M (1999) Effects of visual and leg proprioceptor inputs on recovery of eyestalk posture following unilateral statolith removal in the crayfish. Naturwissenschaften 86: 346–349

Sakuraba T, Takahata M (2000) Motor pattern changes during central compensation of eyestalk posture after unilateral statolith removal in crayfish. Zool Sci 17:19–26

Schaefer KP, Meyer DL, Wilhelms G (1979) Somatosensory and cerebellar influences on compensation of labyrinthine lesions. Prog Brain Res 50: 591-598

Siegler MVS (1981) Postural changes alter synaptic interactions between nonspiking interneurons and motor neurons in the locust. J Neurophysiol 46: 310-323

Schöne H (1954) Statozystenfunktion und statische Lageorientierungbei dekapoden Krebsen. Z Vergl Physiol 36: 241–260

Schöne H (1971) Gravity receptors and gravity orientation in crustacea: In: Gordon SA,

Cohen MJ (ed) Gravity and the Organism. Chicago University Press, Chicago, pp 223–236

Silvey GE, Sandeman DC (1976) Integration between statocyst sensory neurons and oculomotor neurons in the crab *Scylla serrata* III. The sensory to motor synapse. J Comp Physiol 108: 53-65

Smith PF, Darlington CL, Curthoys IS (1986) The effect of visual deprivation on vestibular compensation in the guinea pig. Brain Res 364: 195-198

Smith PF, Curthoys IS (1988a) Neuronal activity in the contralateral medial vestibular nucleus of the guinea pig following unilateral labyrinthectomy. Brain Res 444: 295-307

Smith PF, Curthoys IS (1988b) Neuronal activity in the ipsilateral medial vestibular nucleus of the guinea pig following unilateral labyrinthectomy. Brain Res 444: 308-319.

Smith PF, Curthoys IS (1989) Mechanisms of recovery from unilateral labyrinthectomy. Brain Res Revs 14: 155-180

Stewart WW (1978) Functional connection between cells as revealed by dye-coupling with a highly fluorescent naphthalimide tracer. Cell 14: 741-759

Sugawara K, Hisada M, Higuchi T (1971) Eyestalk musculature of the crayfish, *Procambarus Clarkii*. J Fac Sci Hokkaido Univ Ser VI Zool 18(1):45-50

Van Harreveld A (1936) A physiological solutions for fresh water crustaceans. Proc Soc Exp Biol Med 34:428-432

Vibert N, Bantikyan A, Babalian A, Serafin M, Muhlethaler M, Vidal PP (1999). Post-lesional plasticity in the central nervous system of the guinea pig: a `top-down' adaptation process ? Neurosci 94: 1-5

Wiersma CAG, Yamaguchi T (1967) Integration of visual stimuli by the crayfish central nervous system. J Exp Biol 47:409-431

Williamson R (1989) Secondary hair cells and afferent neurones of the squid statocyst receive both inhibitory and excitatory efferent inputs. J Comp Physiol 165: 847-860

Wilson WA, Goldner MM (1975) Voltage clamping with a single microelectrode. J Neurobiol 6:411-422.

Yamaguchi T, Okada Y (1990) Giant brain neurons of the crayfish: their functional roles in the compensatory oculomotor system. In: Wiese K, Krenz WD, Tautz J, Reichert H, Mulloney B (ed). Frontiers in Crustacean Neurobiology. Birkhäuser, Basel, pp 193–199

Yoshino M, Kondoh Y, Hisada M (1983) Projection of statocyst sensory neurons associated with crescent hairs in the crayfish *Procambarus Clarkii* Girard. Cell Tissue Res 230: 37-48

Figure 1 Physiological and morphological characteristics of NGIs. **A:** Dendrites of NGIs in the protocerebrum. A pair of NGIs are shown schematically. Their cell bodies are located in one of the eyestalk ganglia (not shown). **B:** An NGI stained intracellularly by Lucifer yellow. The main dendrite on the midline and secondary processes in the protocerebrum are shown. **C:** Spontaneous discrete synaptic activities of an NGI recorded from the main dendrite. Two representative traces are shown. **D:** Effects of intracellular current injection into an NGI on the eyecup-up muscle activity. The continuous current clamp mode was chosen in current injection experiments. Due to large current injection (±20nA), the bridge balance could be adjusted only partially so that the membrane potential during current injection could not be recorded. **E:** Schematic diagram showing the presynaptic and postsynaptic connections of NGIs. The whole circuit was compiled from Okada et al. (1994) and modified according to the results in this study. EUM: eyecup-up muscle, EUMN: motor neurons innervating the eyecup-up muscle. NGI: nonspiking giant interneuron, ST: statocyst afferents. Dotted lines indicate polysynaptic pathways.

Figure 2 Effects of statolith removal on the membrane potential of NGIs. **A:** Statolith removal by water jet on the side opposite to the cell body of the recorded NGI. Since the water jet was applied manually, its intensity could not be controlled. The stimulus monitor (lower trace) indicates the duration of water current application. **B:** Statolith removal on the same side with the cell body. The upward deflection in the membrane potential (upper trace) during water jet application is a mechanical artifact. Dashed lines in A and B were obtained from different animals and indicate the resting potential level prior to statolith

removal on the contralateral and ipsilateral side respectively. **C:** Membrane conductance change due to statolith removal on the contralateral side. Constant current pulses (-1 nA) were injected throughout the experiment. The inset shows the membrane potential change in response to current injection before (gray) and after (black) the statolith removal superimposed for comparison.

Figure 3 Comparison of the resting potential of NGIs during the central compensation. The left hatched columns indicate the measurement from NGIs on the right and left side in intact animals. Since the measured values were not different statistically between two sides, they were pooled for the following comparison. The middle and right columns indicate the measurement on the operated and intact side respectively. For both sides, the measurements from intact animals (filled column), those one hour after operation (dark-gray stippled), recovered (light-gray stippled) and non-recovered (open) animals after 14 days after operation are compared. No significant difference was found in any comparison.

Figure 4 Comparison of passive membrane properties of NGIs during the central compensation. **A1-3:** Voltage responses of NGIs to depolarizing and hyperpolarizing current pulses injected and recorded in the main dendrite on the midline. Typical responses of intact (A1), recovered (A2) and non-recovered (A3) animals are shown. **B:** Comparison of the input resistance of NGIs during the central compensation. The left hatched columns indicate the measurement from NGIs on the right and left side in intact animals. Since the measured values were not different statistically between two sides, they were pooled for

the following comparison. The middle and right columns indicate the measurement on the operated and intact side respectively. For both sides, the measurements from intact animals (filled column), those one hour after operation (dark-gray stippled), recovered (light-gray stippled) and non-recovered (open) animals after 14 days after operation are compared. The asterisk indicates the statistically significant difference ($P < 0.05$). **C:** Comparison of the membrane time constant of NGIs during the central compensation. Conventions are the same as in B.

Figure 5 Comparison of spontaneous synaptic activities of NGIs during the central compensation. **A1-2:** Typical records showing the spontaneous discrete PSPs before and after the statolith removal. The statolith was removed on the side contalateral (A1) and ipsilateral (A2) to the cell body of the recorded NGI. A1 and A2 were obtained from different animals. Top two traces are obtained before operation and bottom two just after operation. **B:** Comparison of depolarizing PSP frequencies during the central compensation. The left hatched columns indicate the measurement from NGIs on the right and left side in intact animals. Since the measured values were not different statistically between two sides, they were pooled for the following comparison. The middle and right columns indicate the measurement on the operated and intact side respectively. For both sides, the measurements from intact animals (filled column), those one hour after operation (dark-gray stippled), recovered (light-gray stippled) and non-recovered (open) animals after 14 days after operation are compared. Asterisks indicate statistically significant differences ($P < 0.05$). **C:** Comparison of hyperpolarizing PSP frequencies during the central compensation. Conventions are the same as in B.

Figure 6 Comparison of shape indices for discrete PSPs of NGIs during the central compensation. **A1-2:** Peak amplitude of depolarizing (A1) and hyperpolarizing (A2) PSPs on the operated and intact side. Measurements from intact animals (filled column), those one hour after operation (dark-gray stippled), recovered (light-gray stippled) and non-recovered (open) animals after 14 days after operation are compared. Asterisks indicate statistically significant differences ($P < 0.05$). **B1-2:** Rise rate of depolarizing (B1) and hyperpolarizing (B2) PSPs on the operated and intact side. **C1-2:** Half decay time of depolarizing (C1) and hyperpolarizing (C2) PSPs on the operated and intact side. Conventions are the same as in A.

Figure 7 Schematic summary of obtained results. Changes in the eyestalk posture, passive membrane properties and synaptic activities during the central compensation are diagrammatically recapitulated for intact animals, those 1 hour after operation, and recovered and non-recovered animals 14 days after operation. The figures in light gray on the eyestalk posture row show the symmetrical configuration of intact animals for comparison. The passive membrane properties and synaptic activities 1 hour after operation are compared with the values in intact animals whereas those 14 days after operation are compared with those 1 hour after operation. Upward and downward arrows in parentheses indicate the tendency of increase and decrease respectively with no statistical significance ($P > 0.05$). The upward arrow without parentheses indicates a statistically significant increase ($P < 0.05$). The frequency of PSPs is summarized for excitatory and inhibitory inputs from the viewpoint of whether they are bilaterally balanced

or not.

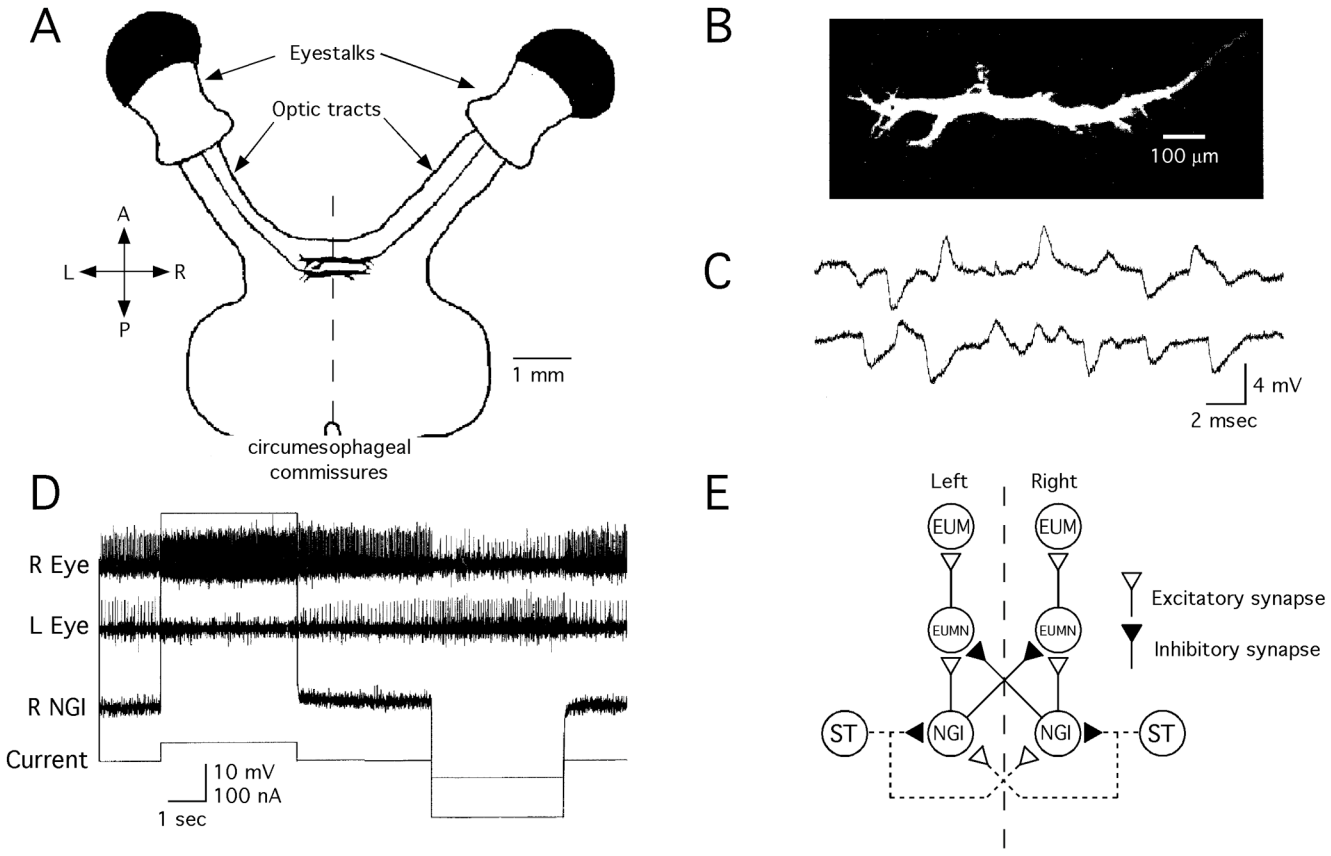

Figure 1 Fujisawa and Takahata

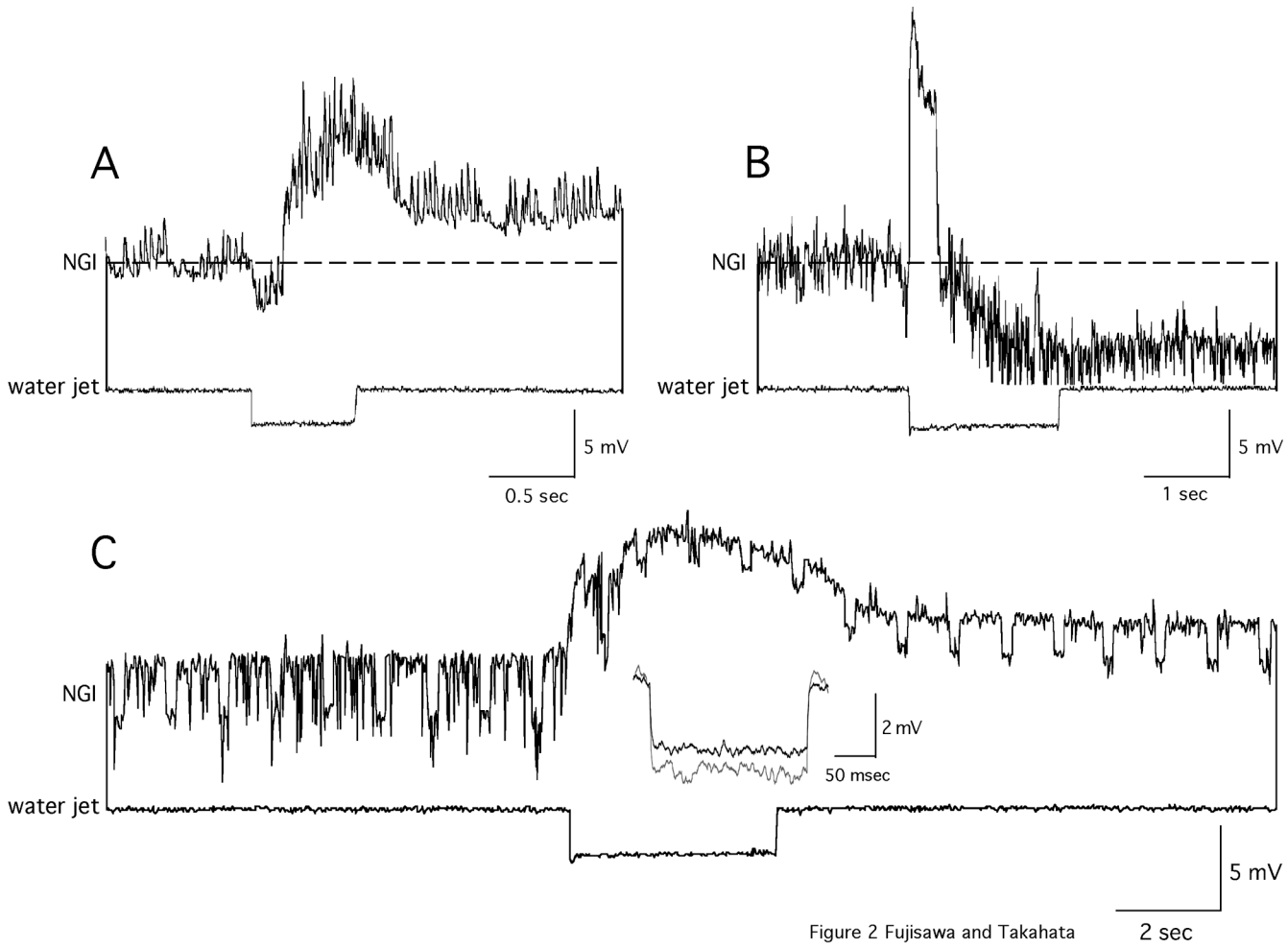

Figure 2 Fujisawa and Takahata

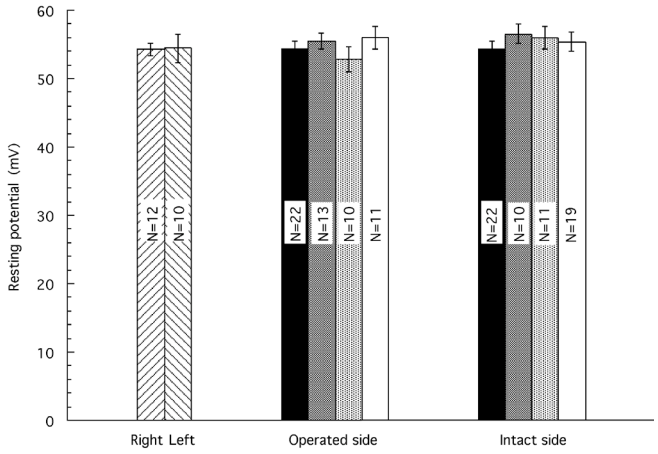

Figure 3 Fujisawa and Takahata

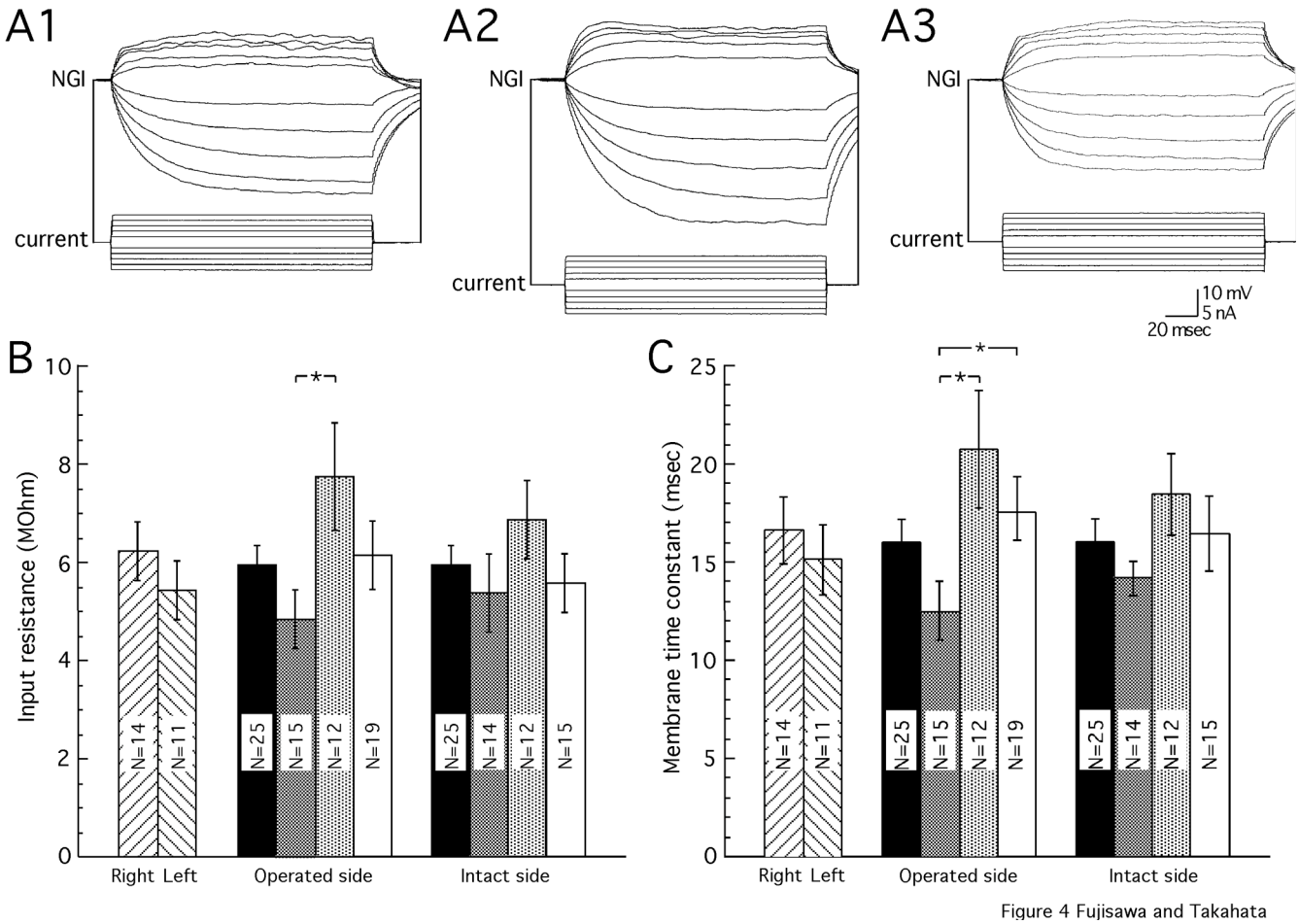

Figure 4 Fujisawa and Takahata

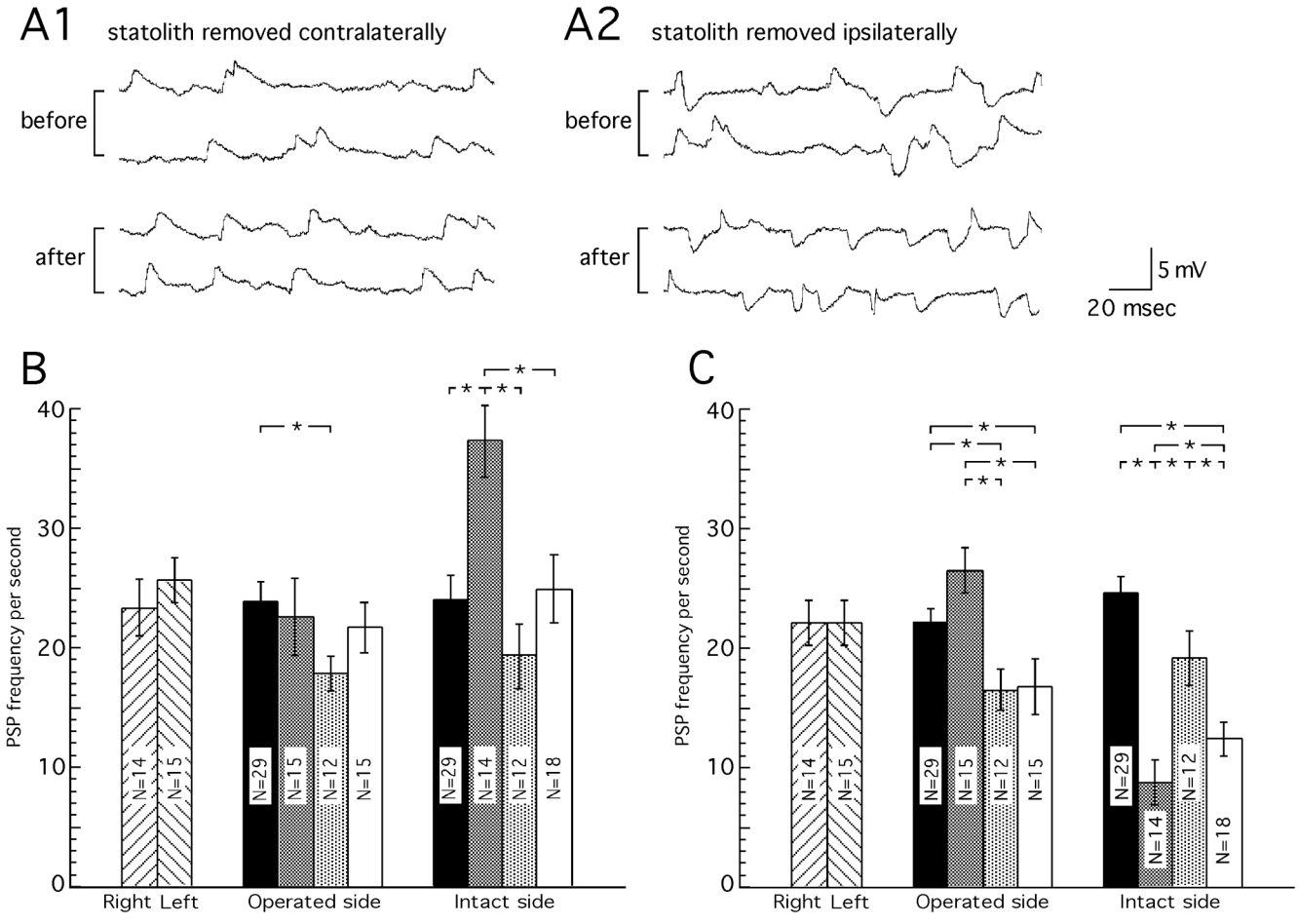

Figure 5 Fujisawa and Takahata

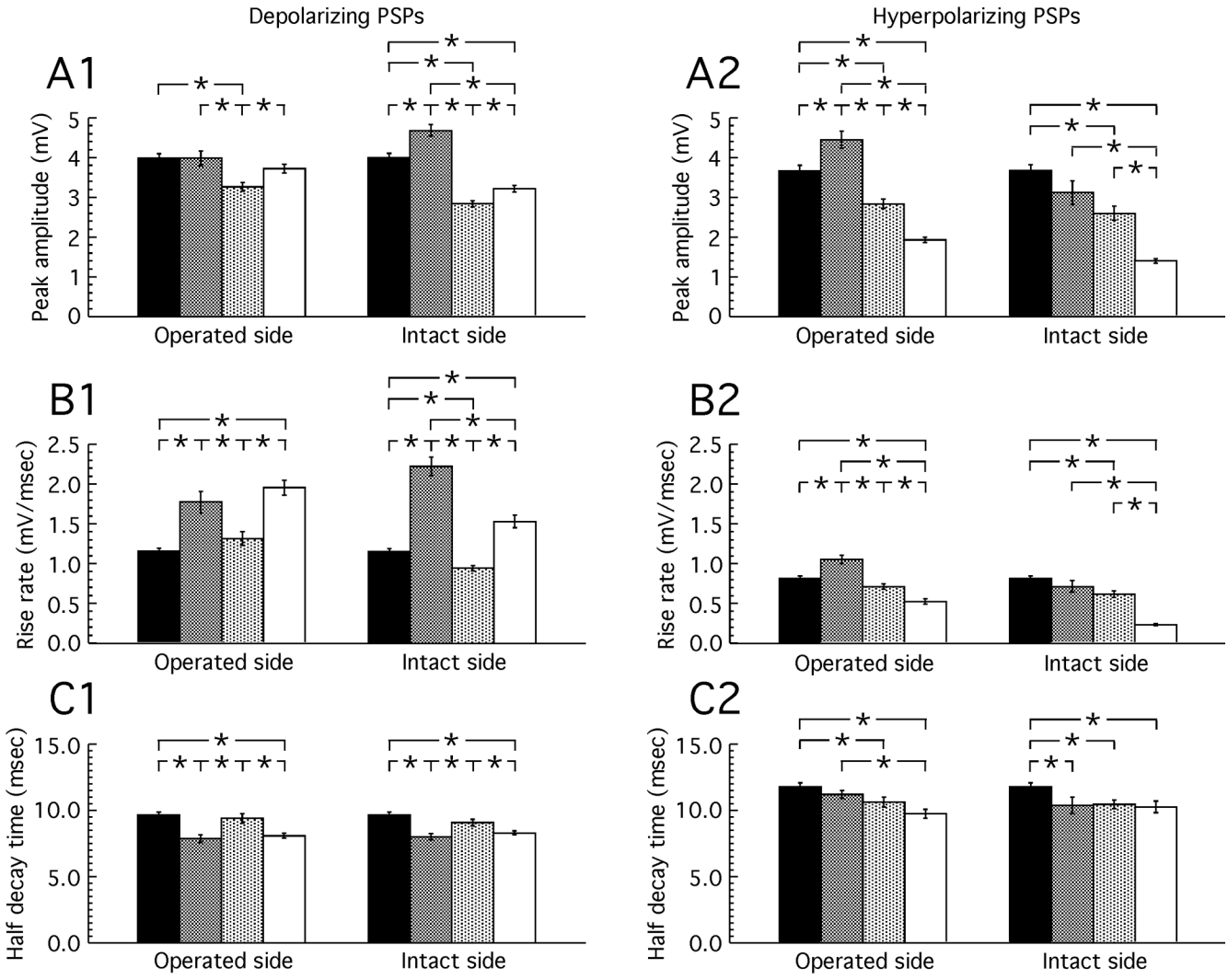

Figure 6 Fujisawa and Takahata

	Intact	1 hour after operation		14 days after operation			
				Recovered		Non-recovered	
		Operated side	Intact side	Operated side	Intact side	Operated side	Intact side
	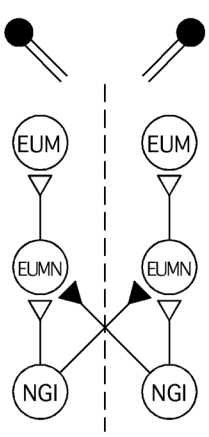	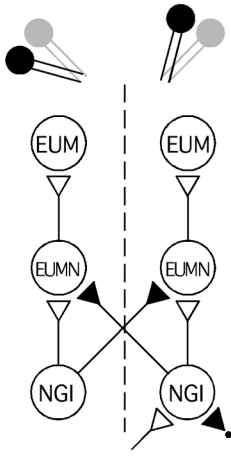		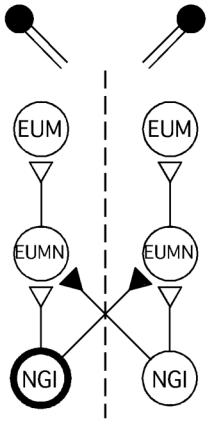		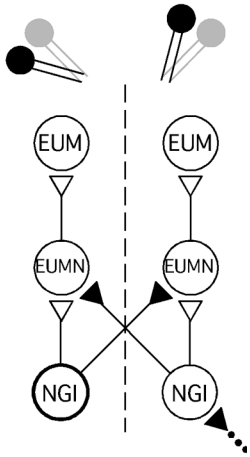	
Input resistance	—	—	(↓)	(↓)	↑	(↑)	(↑)	-
Time constant	—	—	(↓)	(↓)	↑	(↑)	↑	(↑)
Excitatory input	balanced		<		balanced		balanced	
Inhibitory input	balanced		>		balanced		>	

Figure 7 Fujisawa and Takahata